Quantum-Chemistry-Based Force Field for 1,2-Dimethoxyethane and Poly(ethylene oxide) in Aqueous Solution

Dmitry Bedrov, Matthew Pekny,† and Grant D. Smith*

Department of Materials Science and Engineering and Department of Chemical and Fuels Engineering, University of Utah, Salt Lake City, Utah 84112

Received: August 4, 1997; In Final Form: November 10, 1997

An atomistic force field for simulations of 1,2-dimethoxyethane (DME) and poly(ethylene oxide) (PEO) in aqueous solution is presented. The force field is parametrized to reproduce energies of complexes of DME and water as determined from high-level quantum chemistry calculations. The quantum chemistry calculations reveal that the binding of DME to water is comparable to water−water binding in water dimer, indicating strong hydrogen bonding between DME and water. We find that the binding energy of water to DME in the *tgt* conformation (−7.7 kcal/mol) is greater than that for the other low energy DME conformers (−6.1 kcal/mol for *ttt* and −6.4 kcal/mol for tg^+g^- respectively), due to the strong interaction of the water hydrogen atoms with both ether oxygen atoms in the *tgt* conformer. The accuracy of the force field is verified through a series of molecular dynamics simulations of DME−water solutions performed as a function of temperature and composition. Comparison of simulation values for density, excess volume, and viscosity with experiment indicate excellent agreement. Initial analysis of the calculated conformer populations as a function of composition reveals a strong preference for the *tgt* conformer in aqueous solution, and analysis of the pair distribution functions appears to be consistent with suggestions that this is due to the compatibility of the DME *tgt* geometry with the structure of liquid water.

Introduction

Poly(ethylene oxide) (PEO) is of great scientific and technological interest for a wide variety of applications, many of which depend upon the properties of the polymer in aqueous solution.[1] Extensive calorimetry, scattering, and spectroscopy studies of PEO in aqueous solution (e.g., ref 2−5) have led to different, and often contradictory, pictures of the polymer conformations, hydration, and the observed phase equilibrium behavior. We believe that a much clearer understanding of the PEO properties in aqueous solution can be gained through careful, detailed modeling studies carried out at the atomistic level.

The ability of computer simulations to describe the behavior of a material depends critically upon the accuracy of the inter- and intramolecular potential energy functions, or force field, for the system of interest. In this work, we present a force field for simulations of 1,2-dimethoxyethane (DME) in aqueous solution, a model system for PEO−water solutions, and also present results of molecular dynamics simulations of DME−water solutions as a function of composition and temperature. In future work, we will present a more detailed analysis of the DME−water simulations, and we will employ this force field in simulations of PEO−water solutions to better understand the thermodynamic, phase equilibrium, and structural properties of this important system.

Force Field Development

Two principal strategies are employed in obtaining the potential energy functions for materials simulations. The first is to base development of the force field purely upon empirical data. In this approach the force field is parametrized to provide the best description of experimental data for model systems, such as pair distribution functions obtained from scattering or thermodynamic properties. Such data are almost always insufficient to allow complete parametrization of a force field, particularly for systems containing conformationally flexible molecules. Even where sufficient experimental data exists to parametrize a force field, it is often the case that the parameters which "best" describe the available data are not unique.

The second method of constructing the atomistic potential is to augment experimental data with calculated molecular geometries, vibrational frequencies, conformational energies, charge distributions, and intermolecular interaction energies. In this approach, ab initio electronic structure, or quantum chemistry, calculations are usually preferable over less computationally intensive but less reliable semiempirical methods, unless the accuracy of the latter has been thoroughly demonstrated for the specific system of interest (usually through comparison with high-level ab initio calculations or experiment). In previous work we have parametrized force fields for pure DME[6] and for interactions of DME with lithium salts,[7] based largely upon quantum chemistry calculations. Subsequently, we have employed these force fields in simulations of DME liquid,[8] pure PEO melts,[9,10] and PEO−LiI solutions.[11,12] In each case, simulations employing our quantum-chemistry-based force fields have yielded excellent agreement with a wide variety of experimental structural, dynamic, and thermodynamic data.

The primary purpose of this work is to develop an accurate, validated atomistic description of ether−water interactions for use in classical atomistic molecular dynamics simulations. Although a number of modeling studies of ethers in aqueous solution have already been conducted, the need for such a

† Current Address: Department of Chemical Engineering, University of Colorado.

* To whom correspondence should be addressed.

S1089-5647(97)02545-5 CCC: $15.00
Published on Web 01/22/1998

potential remains. Three different simulation techniques have been applied in the study of ethers in aqueous solutions. The first involves the so-called QM/MM methods.[13−15] These methods combine a classical atomistic molecular mechanics potential for the solvent−solvent interaction and semiempirical quantum mechanical calculations of the solute−solvent interactions. The second method employs an implicit solvent model[16] in treating solute−solvent interactions. Classical atomistic molecular dynamics simulations, which do require atomistic potentials for solute−solvent interactions, have been performed on polyethers and crown ethers in aqueous solution (e.g., refs 17−19). None of these approaches has involved development of an accurate, atomistic potential for ether−water interactions. The QM/MM and implicit solvent models do not utilize atomistic descriptions of the interactions between the solute and solvent. The molecular dynamics simulations of the ether−water systems performed to date have used "standard" atomistic force fields[20] to describe the ether−ether and water−water interactions and generic combining rules to describe ether−water interactions. As we demonstrate below, combining rules in general will not yield an accurate description of ether−water interactions.

DME−Water Interactions. In the study DME and PEO in aqueous solution, we will employ our validated quantum-chemistry-based force field for DME[6] to describe DME−DME (and polymer−polymer) interactions and the TIP4P (four-point transferable intermolecular potential) model[21] for water−water interactions. Therefore, to perform simulations of the DME or PEO in aqueous solution, we need to obtain force field parameters only for the ether−water interactions. In the simplest description, the interaction between a DME molecule and a TIP4P water molecule consists of electrostatic interactions among the carbon, hydrogen, and oxygen atoms comprising DME and the hydrogen atoms and oxygen charge center of the TIP4P water and the repulsion−dispersion interactions between the atoms comprising DME and the nonbonded force center of the TIP4P water located on the oxygen atom. The partial atomic charges for both DME[6] and water[21] have been determined previously. If we use a Lennard-Jones description for the repulsion−dispersion interactions, we must establish the values of the six unknown nonbonded force field parameters ϵ_{c-w}, σ_{c-w}, ϵ_{o-w}, σ_{o-w}, ϵ_{h-w}, and σ_{h-w} employed in the expression

$$E_{i-w} = 4\epsilon_{i-w}[(\sigma_{i-w}/r_{i-w})^{12} - (\sigma_{i-w}/r_{i-w})^{6}] \qquad (1)$$

where i = carbon, hydrogen, or oxygen (DME) and r_{i-w} is the separations between an atom comprising DME and the water nonbonded force center (oxygen atom). In this representation, the parameter ϵ gives the energy of maximum attraction for a given pair, and σ gives the separation at the point of zero energy. To reduce the number of unknown force field parameters, we have taken the following approach. We obtained initial values for the six parameters using standard geometric mean combining rules:

$$\epsilon^{o}_{i-w} = \sqrt{\epsilon_{i-i}\epsilon_{w-w}} \qquad \text{and } \sigma^{o}_{i-w} = \sqrt{\sigma_{i-i}\sigma_{w-w}} \qquad (2)$$

These values are shown in Table 1. Also shown are the values of ϵ and σ for DME and water used in obtaining these initial values. We then adjusted the DME−water parameters according to

$$\epsilon_{i-w} = \alpha[\epsilon^{o}_{i-w}] \qquad \text{and } \sigma_{i-w} = \beta[\sigma^{o}_{i-w}] \qquad (3)$$

yielding just two adjustable parameters, α and β. Values for α and β were determined in two different ways, described briefly here and in greater detail below. The first method involved adjusting the parameters, such that the experimental density of DME−water as a function of composition and temperature, was well reproduced via molecular dynamics simulations. The second involved fitting quantum chemistry values for the binding energy of a DME−water complex as a function of complex geometry. The resulting force field parameters are given in Table 1.

TABLE 1: Lennard-Jones Parameters for DME−Water Interactions DME[a] and Water[b]

DME[a] and Water[b]						
interaction	ϵ (kcal/mol)		σ Å			
C−C	0.0950		3.4477			
O−O	0.2000		2.8509			
H−H	0.0098		3.0025			
W−W	0.1550		3.1540			
DME−Water[c]						
interaction	ϵ^0 (kcal/mol)	σ^0 (Å)	ϵ^{emp} (kcal/mol)	σ^{emp} (Å)	ϵ^{qc} (kcal/mol)	σ^{qc} (Å)
W−C	0.1214	3.2975	0.1927	3.1730	0.2405	3.2665
W−O	0.1761	2.9986	0.2795	2.8853	0.3490	2.9704
W-H	0.0390	3.0773	0.0619	2.9610	0.0772	3.0484

[a] A Lennard-Jones representation of the exp-6 interactions in ref 6. [b] Reference 13. [c] "$_0$" = initial values from geometric mean combining rules: "*emp*" = empirical force field, "*qc*" quantum-chemistry-based force field.

Empirical DME−Water Force Field

Our initial approach in obtaining a DME−water force field involved adjusting the α and β scaling parameters in eq 3 such that the density of the DME−water solutions as a function of temperature and composition predicted by molecular dynamics simulations were in good agreement with experimental values.[22,23] Details of the molecular dynamics simulation methodology are given below. The initial values for the force field parameters ($\alpha = \beta = 1$), obtained from standard combining rules, yielded an immiscible DME−water system. Such behavior is consistent with a force field that underestimates the attraction between DME and water. Consequently, we adjusted α and β such that the repulsive term of the Lennard-Jones energy (the first term in eq 1) remained unchanged, while the attractive dispersion energy (second term) was allowed to increase until miscibility and good representation of the density data were achieved for all compositions. The good agreement between the simulations and experiment using this force field is shown in Figure 1 at 45 °C. Nearly identical agreement is obtained at 25 °C (not shown) indicating that the thermal expansion is well represented over the limited temperature range of the experimental data.

Quantum-Chemistry-Based DME−Water Force Field

We have investigated the interactions of DME and water by performing high-level quantum chemistry calculations on a DME + water complex as a function of DME conformation and complex geometry. The influence of the level of theory employed on the quantum chemistry results is discussed below. The minimum energy geometries of *tgt*, *ttt*, and tg^+g^- DME−water complexes are illustrated in Figure 2. We performed all geometry optimizations at the SCF level using a D95** basis set, as in our previous studies of DME[24] and DME−LiI[7] complexes. The internal geometries of DME and water in the *tgt* DME−water complex are given in Table 2, along with the

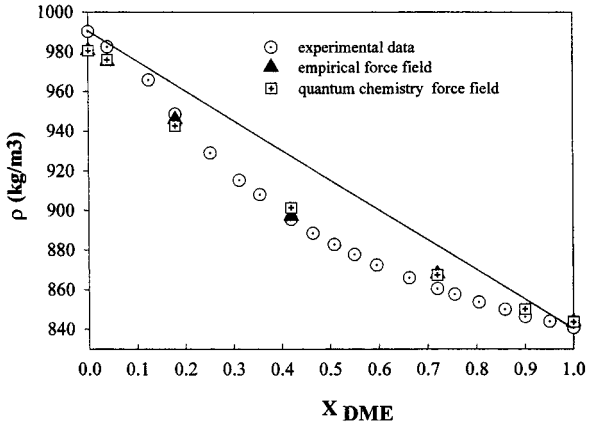

Figure 1. Density of DME−water solution as a function of composition at 45 °C. The solid line shows the ideal solution density.

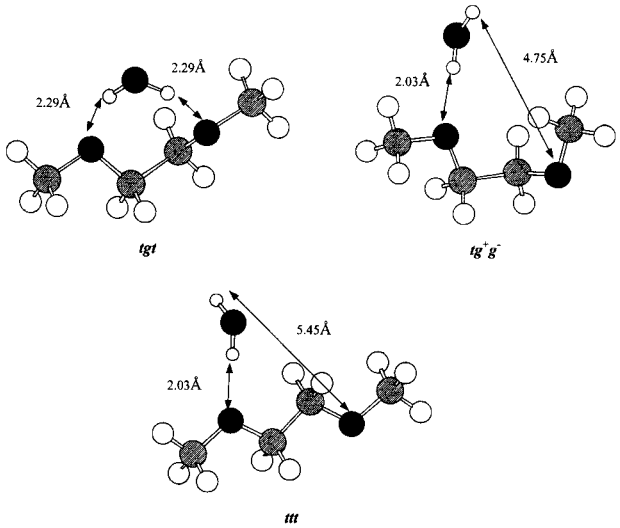

Figure 2. Optimized geometries for the *tgt*, *ttt*, and tg^+g^- DME−water complexes. Distances indicate the closest $O_{DME}-H_w$ approaches.

TABLE 2: Internal Geometries[a] of *tgt* DME−Water

	tgt + water	*tgt* alone	water alone
torsions			
C−O−C−C	177.2	184.6	
O−C−C−O	74.3	73.6	
angles			
C−O−C	113.7	114.0	
O−C−C	110.2	109.7	
$H_w-O_w-H_w$	103.1		106.8
bond lengths [Å]			
C−O	1.399	1.394	
O−C	1.399	1.395	
C−C	1.512	1.512	
H_w-O_w	0.946		0.944

[a] All geometries are from SCF optimization using a D95** basis set.

relaxed geometries of the ether and water obtained at infinite separation. The formation of the complexes results in minimal distortion of the ether or water. This is in stark contrast to the ether−Li^+ complexes, where significant distortion of the ether was seen.[7]

We have determined the DME−water binding energies at several levels of theory by subtracting the calculated energies of the isolated ether and water in their (slightly) distorted complex geometries from the calculated energy of the complex at the optimized geometries. The resulting binding energies are shown in Table 3 for the D95** and D95+(2df,p) basis

TABLE 3: Quantum Chemistry Binding Energies for Optimized[a] DME−Water Complexes

conformation	D95** (SCF)	D95** (MP2)	D95+(2df,p) (SCF)	D95+(2df,p) (MP2)
ttt	−4.85	−6.86	−3.83	−6.06
tg^+g^-	−4.68	−7.05	−3.66	−6.36
tgt	−6.53	−8.99	−4.88	−7.67

[a] All geometries are from SCF/D95** optimizations.

TABLE 4: Influence of Level of Theory on the Binding Energy for the *tgt* DME/Water Complex[a]

	without BSSE		with BSSE[b]	
basis set	SCF	MP2	SCF	MP2
D95*	−6.71	−9.32	−5.33	−5.50
D95**	−6.53	−8.99	−5.28	−5.29
D95+(2df,p)	−4.88	−7.67	−4.33	−5.28

[a] All geometries are from SCF/D95** optimizations. [b] Using counterpoise method.

sets (D95** SCF geometries) at both the SCF and MP2 levels for the three lowest energy DME conformers. At all levels of theory, the DME−water interaction is stronger for the *tgt* conformer, analogous to the much stronger binding of Li^+ to *tgt* DME.[7] In the *tgt* conformer, the oxygen atoms are arrayed such as to allow hydrogen bonding with both water hydrogen atoms. The closest water hydrogen−ether oxygen distances are shown in Figure 2.

Level of Theory. Our previous studies of model ethers indicate that MP2 level calculation employing a D95+(2df,p) basis set yield accurate conformational energies.[24−26] Calculations at a similar level of theory yielded accurate binding energies for ether−Li^+ complexes.[7] On the other hand, our studies of the binding of benzene dimer indicate that larger basis sets should be employed if the dispersion energy, which is important for the benzene dimer, is to be accurately represented.[27] When basis set superposition effects were neglected, a more modest basis set was capable of describing the binding in benzene dimer reasonably well.[27] In general, accurate determination of complex energies is more difficult than determining relative conformational energies because of the importance of dispersion effects in the former. Such calculations require large basis sets with multiple diffuse and polarization functions.

A study of the *tgt* DME−water complex as a function of basis set size, electron correlation, and basis set superposition error is shown in Table 4. Unlike the case for benzene dimer,[27] we could discern no clear trend indicating what level of calculation might yield the most accurate binding energies. In addition, we could find no experimental data on the binding of DME and water. As a result, we turned to water dimer as a model system. Water dimer has been the subject of extensive ab initio studies (e.g., refs 28, 29). After a review of these efforts, we performed our own investigation of the influence of basis set size, electron correlation treatment, and basis set superposition effects on the geometry and energy of water dimer. Our purpose was to determine a level of theory that could accurately reproduce experiment data for water dimer while being modest enough to allow application to a large number of DME−water complex geometries. We found that geometry optimization performed a D95** basis set at the SCF level, and MP2 energies at the D95+(2df,p) level (without BSSE corrections) using this geometry, yield a geometry and energy for water dimer in good agreement with experiment[30,31] as summarized in Table 5. Consequently, we performed our study of DME−water complexes at this level of theory, which is

TABLE 5: Water Dimer Properties

property	experiment[a]	quantum chemistry[b]
O−O separation (Å)	2.980 ± 0.004	2.98
binding energy (kcal/mol)	−5.4 ± 0.7	−5.5
Θ_A[c]	57 ± 10	47
Θ_D[c]	−51 ± 10	−56

[a] References 30 and 31. [b] SCF/D95**//MP2/D95+(2df,p). [c] Angle of the bisector of the H−O−H angle of the acceptor (A) or donator (D) water with respect to the O−H−O hydrogen bond.

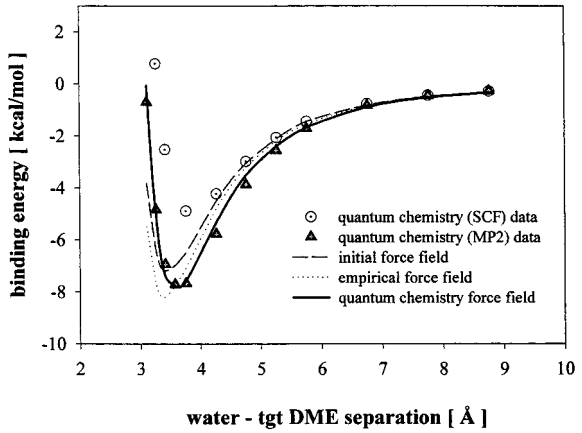

Figure 3. Binding Energy in the *tgt* DME−water complex as a function of separation.

consistent with our previous studies of ethers and ether complexes as described above.

DME−Water Energies. The binding energy of *tgt* DME and water as a function of the distance between the midpoint of the DME C−C bond and the water oxygen is shown in Figure 3. For these calculations, DME and water were maintained in their minimum energy complex (r = 3.76 Å) geometries and orientation, and the separation was systematically increased and decreased. The large difference between the SCF and MP2 energies indicates the importance of including electron correlation effects, and reveals that dispersion effects contribute significantly to the complex energies. The water hydrogen−DME oxygen distances in the minimum energy complex (Figure 2) are similar to that found in the water dimer (2.03 Å), indicating strong hydrogen bonding.

Polarization Effects. Before proceeding to adjust the force field to fit the DME−water binding energies, we wished to determine if polarization, or induction, effects, are important in the interaction of water and DME. The simple two-body Coulomb + dispersion−repulsion potential does not account for induction effects. It was found in DME−Li^+ complexes that induction effects are quite important, and it was necessary to augment the potential energy functions to account for these interactions.[7] The procedure used to investigate the importance of polarization effects is illustrated in Figure 4. A second water molecule was added to the minimum energy DME−water complex on the opposite side of the DME molecule, with the same C−C midpoint/oxygen separation as the first water. The dipole moment of the second water is collinear with, but in opposite direction to that of the first water. The geometry and energy (at the MP2/D95** level) for the three molecule complex are shown in Figure 4. In addition, we determined the energies of the three two molecule complexes illustrated in Figure 4. These complex energies, along with their sum, are also given in Figure 4. If polarization effects (i.e., interactions of the water dipole moments with induced dipole moments in DME) are important, we would expect the total binding in the three two

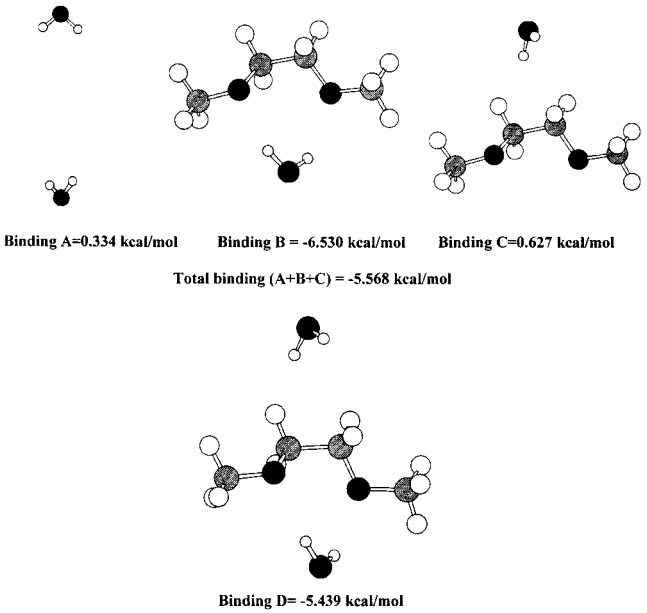

Figure 4. Investigation of polarization effects in DME−water interactions.

molecule complexes to be greater than that in the three molecule complex. As this is not the case, we conclude that polarization effects do not play an important role in the interaction of DME and water.

Force Field. Adjustment of α and β to yield the best agreement with quantum chemistry for the complex energies given in Figure 3 yields the force field parameters given in Table 1. Fitting of the parameters was accomplished using standard nonlinear least-squares techniques, with greater weight being placed on representing the complex energies near the optimal geometry. Agreement between the force field and quantum chemistry is excellent as can be seen in Figure 3. Because of the difficulties involved in determining accurate absolute intermolecular energies from ab initio methods, we considered the possibility that the quantum chemistry force field might require further "empirical" adjustment. We planned on making any required adjustments in the force field in such a manner that position of the minimum energy of the of the DME−water complex remained unchanged, as we believe position of the minimum energy is more reliable than the value of the energy itself. As will be discussed below, it was unnecessary to make any such adjustments to the quantum-chemistry-based force field.

The complex energies yielded by the initial force field and the empirical force field are also shown in Figure 3. The initial force field yields a much weaker interaction between DME and water, consistent with the immiscibility of the species when this force field is utilized. Interestingly, despite that fact that the empirical force field gives a good representation of the density as a function of composition and temperature (Figure 1), the interaction between DME and water is significantly different than that predicted by our quantum chemistry calculations. The minimum energy complex occurs at a shorter separation with the empirical force field (3.42 vs 3.76 Å), and the interaction at larger separations the DME−water interaction is less favorable.

Molecular Dynamics Simulations

Molecular dynamics simulations of DME−water systems as a function of temperature and composition were employed to

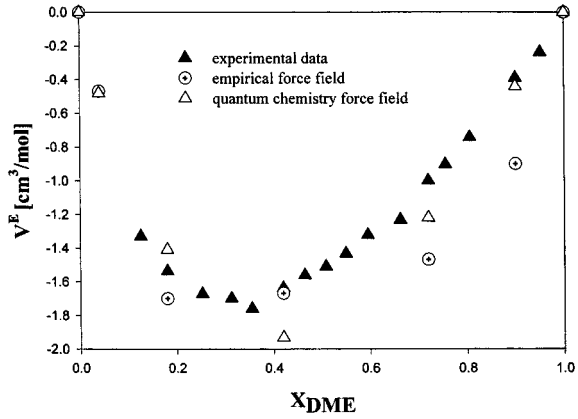

Figure 5. Excess volume of DME−water solutions as a function of composition. Values are at 45 °C.

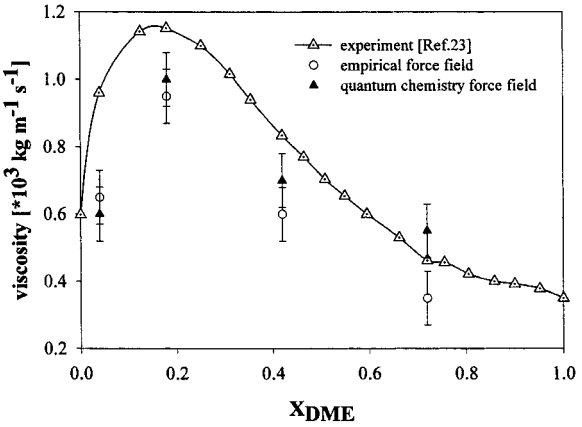

Figure 6. Viscosity of DME−water solutions as a function of composition. Values are at 45 °C.

test both the empirical and quantum chemistry force fields. The simulations were performed using the constant temperature−pressure methods[32] implemented as described elsewhere.[33] Five DME−water systems, with compositions $x_{DME} = 0.032$, 0.180, 0.420, 0.720, and 0.900, were investigated. Simulations were performed at 25 and 45 °C. Each system contained about 1300 atoms. Periodic boundary conditions were employed. Bond lengths were constrained using the standard Shake algorithm, while all other degrees of freedom remained flexible. The Ewald summation[34] method was employed to handle long-range electrostatic effects. The initial systems, consisting of DME and water molecules in a regular array with a greatly reduced density, were equilibrated for 0.1 ns. The density was increased to experimental values over 0.5 ns. Each system was then equilibrated over 0.6 ns. Sampling for each system occurred over 0.4 ns for density calculations and 0.7 ns for viscosity calculations. A time step of 1.0 fs was employed.

Thermodynamic Properties. A comparison of experimental densities (ρ) and excess volume (V^E) data,[22,23] as a function of composition with simulation results is shown in Figures 1 and 5, respectively. Because the empirical force field was parametrized to fit the experimental density data, good agreement with experiment is seen. The quantum chemistry based force field, *without* empirical adjustment, also yields an accurate description of the density. At all compositions, deviation from experiment is less than one percent. As a result, we determined that no adjustment of the quantum chemistry based force field was required.

Experimentally, significant deviation from ideal solution density is seen for the DME−water solutions, as indicated by the difference between the solid line and the experimental points in Figure 1. This difference yields the excess volume, shown in Figure 5. The excess volume has a minimum at a composition of around 0.4. While the force fields yield what appear to be quite similar densities, they in fact give quite different descriptions of the excess volume. The position of the minimum and the shape of the excess volume curve predicted by the quantum-chemistry-based force field is in much better agreement with experiment that predicted by the empirical force field.

Viscosity. The shear viscosity of the solutions was calculated using the Einstein relation[35]

$$2t\eta = \langle (A_{\alpha\beta}(t) - A_{\alpha\beta}(0))^2 \rangle / V k_B T \qquad (4)$$

where

$$A_{\alpha\beta} = \sum_i r_{i\alpha} p_{i\beta} \qquad (5)$$

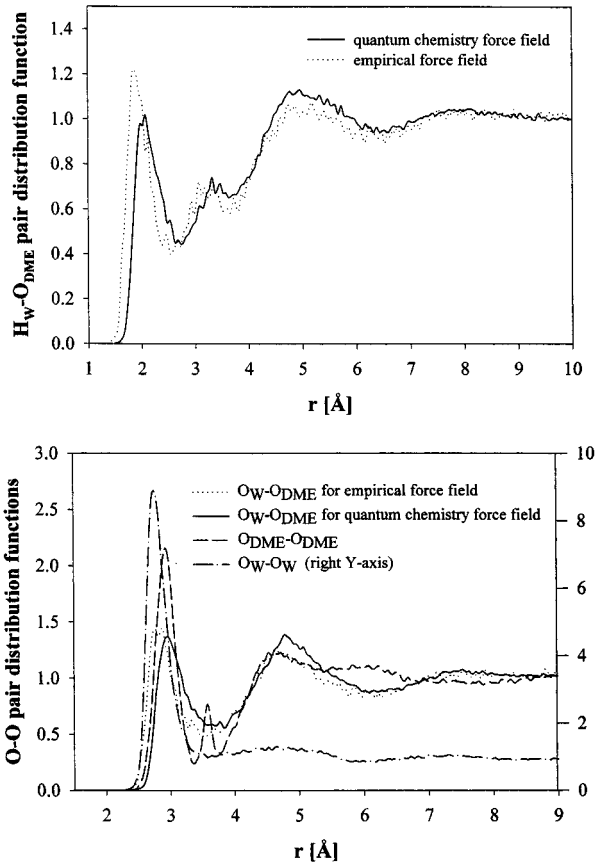

Figure 7. Pair distribution functions for DME−water solutions from molecular dynamics simulations for $X_{DME} = 0.420$. (a) H_w−O_{DME} and (b) O_w−O_w, O_{DME}−O_{DME} (includes intramolecular contribution), and O_w−O_{DME}.

and r_i and p_i are the position and momentum of ith atom, η is the viscosity, t is sampling time, T is temperature, V is the simulation volume, and $\alpha\beta = xy$, yz, zx, etc. The calculated viscosity is less accurate than the excess volume because of inherently lower statistical precision. In Figure 6, the calculated viscosity is compared to experimental values.[22,23] Given the statistical uncertainty in the calculated viscosity, and the fact that reported experimental values can differ by more than 5%, agreement between experiment and simulation using the quantum-chemistry-based force field is reasonable. It is hard to make any conclusion concerning the comparison of accuracy of quantum-chemistry-based and empirical force fields, because of statistical uncertainties in the calculated viscosities. Both

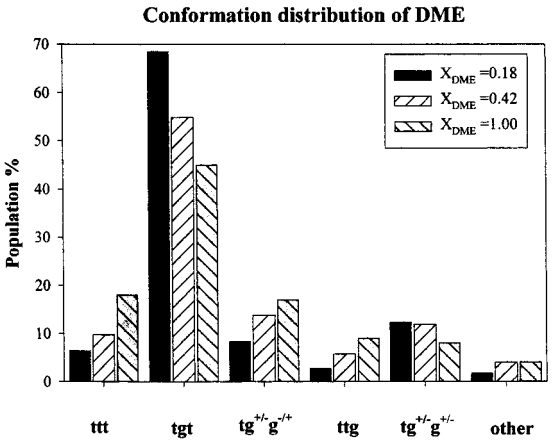

Figure 8. DME Conformer populations in DME−water solution as a function of composition. From simulations at 45 °C.

force fields give qualitatively the right concentration dependence of the viscosity.

Local Structure and Conformer Populations. A detailed discussion of local structure and dynamics in DME−water systems, involving a comparison of X-ray and quasielastic neutron scattering experiments with simulations, is the subject of an upcoming manuscript. Here, we briefly consider the local structure of the DME−water solutions and the influence of concentration on DME conformer populations. Figure 7 shows the H_w-O_{DME} and the various O−O pair distribution functions. The pair distribution functions for both force fields show a first peak in the H_w-O_{DME} pair distribution function indicative of hydrogen bonding. However, the local structure is noticeably different for the different force fields, with the hydrogen bonds being about 0.2 Å shorter for the empirical force field. Differences in the O−O pair distribution functions can also be seen. The X-ray structure factor will be quite sensitive to such differences in local structure.

The distribution of DME conformers as a function of solution composition for the quantum chemistry force field is shown at Figure 8. Our simulation results are consistent with recent Raman spectroscopy experimental data,[36] which observed an apparent increase in the population of *tgt* conformer with increasing water content in the mixture. The investigators[36] associated this stabilization of *tgt* conformer with the structure of liquid water. Our simulation indicate that distance between two oxygen atoms in *tgt* molecule is about 2.95 Å, which is almost the same as the closest oxygen−oxygen distance, 2.85 Å, of liquid water.[28] Our DME−water simulations give the first O_w-O_w intermolecular peak at about 2.78 Å, as shown in Figure 7b. We can see from Figure 7b that the distance of the first O_w-O_{DME} intermolecular peak is also just slightly less than 3 Å. Hence, the gauche DME arrangement appears to fit favorably into the water network. A more detailed analysis of the structure of DME−water solutions is the subject of an upcoming manuscript.

References and Notes

(1) Harris, J. M. *Poly(Ethylene Glycol) Chemistry: Biotechnical and Biomedical Applications*; Plenum Press, NY, 1992.
(2) Matsuura, H.; Fukuhara, K. *J. Mol. Struct.* **1985**, *126*, 251.
(3) Saeki, S.; Kuwahara, N.; Nakata, M.; Kaneko, M. *Polymer* **1976**, *17*, 685.
(4) Breen, J.; Huis, D.; de Bleijser, J.; Leyte, J. C. *J. Chem. Soc., Faraday Trans. 1* **1988**, *84*, 290.
(5) Bieze, T. W. N.; Barnes, A. C.; Huige, C. J. M.; Enderby, J. E.; Leyte, J. C. *J. Phys. Chem.* **1994**, *98*, 6568.
(6) Smith, G. D.; Jaffe, R. L.; Yoon, D. Y. *J. Phys. Chem.* **1993**, *97*, 12752.
(7) Smith, G. D.; Jaffe, R. L.; Partridge, H. *J. Phys. Chem. A* **1997**, *101*, 1705.
(8) Smith, G. D.; Jaffe, R. L.; Yoon, D. Y. *J. Am. Chem. Soc.* **1995**, *117*, 530.
(9) Smith, G. D.; Yoon, D. Y.; Jaffe, R. L, Colby, R. H., Krishnamoorti, R., Fetters, L. J. *Macromolecules* **1996**, *29*, 3462.
(10) Smith, G. D.; Yoon, D. Y.; Wade, C. G.; O'Leary, D.; Chen, A.; Jaffe, R. L. *J. Chem. Phys.* **1997**, *106*, 3798.
(11) Smith, G. D.; Borodin, O.; Pekny, M.; Annis, B.; Londono, D.; Jaffe, R. L. *Spectrachim. Acta. A* **1997**, *53*, 1273.
(12) Londono, J. D.; Annis, B. K.; Habenschuss, A.; Borodin, O.; Smith, G. D.; Turner, J. Z.; Soper, A. K. *Macromolecules*. **1997**, *30*, 7151.
(13) Liu, H.; Müller-Plather, F.; van Gunsteren, W. F. *J. Chem. Phys.* **1995**, *102*, 1722.
(14) Engkvist, O.; Åstrand, P. O.; Karlström, G. *J. Phys. Chem.* **1996**, *100*, 6950.
(15) Engkvist, O.; Karlström, G. *J. Chem. Phys.* **1997**, *106*, 2411.
(16) Williams, D. J.; Hall, K. B. *J. Phys. Chem.* **1996**, *100*, 8224.
(17) Depner, M.; Schürmann, B. L.; Auriemma, F. *Mol. Phys.* **1991**, *74*, 715.
(18) Kong, Y. C.; Nicholson, D.; Parsonage, N. G. *J. Chem. Soc., Faraday Trans.* **1995**, *91*, 4261.
(19) Dang, L. X. *J. Am. Chem. Soc.* **1995**, *117*, 6954.
(20) A number of force fields, such as *AMBER*, Cornell, W. D. *J. Am. Chem. Soc.* **1995**, *117*, 5179−5197; *OPLS*, Jorgensen, W. L.; Tirado-Rives, J. *J. Am. Chem. Soc.* **1988**, *110*, 1657−1666; and *SPC/E*, Berendsen, H. J. C.; Grigera, J. R.; Straatsma, T. P *J. Phys. Chem.* **1987**, *91*, 6269, have been employed in ether−water simulations.
(21) Jorgensen, W. L.; Chandrasekhar, J.; Madura, J. D.; Impey, R. W.; Klein, M. *J. Chem. Phys.* **1983**, *79*, 926.
(22) Douheret, G.; Davis, M. I.; Hernandez, M. E.; Flores, H. *J. Indian Chem. Soc.* **1993**, *70*, 395.
(23) Das, B.; Roy, M. N.; Hazra, D. K. *Indian J. Chem. Technology* **1994**, *1*, 93.
(24) Jaffe, R. L.; Smith, G. D.; Yoon, D. Y. *J. Phys. Chem.* **1993**, *97*, 12745.
(25) Smith, G. D.; Jaffe, R. L, Yoon, D. Y. *J. Chem. Phys.* **1994**, *98*, 9078.
(26) Smith, G. D.; Crain, K.; Jaffe, R. L. *J. Phys. Chem. A* **1997**, *101*, 3152.
(27) Jaffe, R. L.; Smith, G. D. *J. Chem. Phys.* **1996**, *105*, 2780.
(28) Xantheas, S. S., Dunning, T. H., Jr. *J. Chem. Phys.* **1993**, *99*, 8774.
(29) Xantheas, S. S., Dunning, T. H., Jr. *J. Chem. Phys.* **1993**, *98*, 5233.
(30) Odutola, J. A., Dyke, T. R. *J. Chem. Phys.* **1980**, *72*, 5062.
(31) Diercksen, G. H. F.; Kraemer, W. P.; Roos, B. O. *Theor. Chim. Acta* **1975**, *36*, 249.
(32) Nose, S. *J. Chem. Phys.* **1984**, *81*, 511.
(33) Smith, G. D.; Jaffe, R. L.; Yoon, D. Y. *Macromolecules* **1993**, *26*, 298.
(34) Allen, M. P.; Tildesley, D. T. *Computer Simulation of Liquids*; Oxford, NY, 1987.
(35) Haile, J. M. *Molecular Dynamic Simulation*; J. Wiley & Sons: NY, 1992.
(36) Yoshida, H.; Takikawa, K.; Kaneko, I.; Matsuura, H. *J. Mol. Struct.* **1994**, *311*, 205.